

# Lithium perturbation and *gooseoid* expression identify a dorsal specification pathway in the pregastrula zebrafish

Scott E. Stachel<sup>1,†</sup>, David J. Grunwald<sup>1,\*</sup> and Paul Z. Myers<sup>2</sup>

<sup>1</sup>Departments of Human Genetics and <sup>2</sup>Biology, University of Utah, Salt Lake City, UT 84112, USA

\*Author for correspondence

†Current address: Department of Molecular and Cellular Biology, University of California, Berkeley, CA 94720, USA

## SUMMARY

The zebrafish dorsoventral axis can first be distinguished at gastrulation, upon formation of the embryonic shield, the site of the organizer. We have asked whether the shield is specified before gastrulation. First, we show that brief exposure of premidblastula embryos to lithium, which is known to shut down the phosphoinositol signaling pathway, produces excessive shield formation and extreme hyper-dorsal development. Second, we show that the zebrafish *gooseoid* homeobox gene is activated at or just after the midblastula in a localized domain of cells that subsequently populate the most anterior region of the incipient shield and axial

hypoblast. *gooseoid* expression is elevated and radialized by early lithium treatment, suggesting that *gooseoid* plays a role in establishing the organizer and shield. Our results demonstrate that the zebrafish dorsal axis is signaled by a pathway initiated in the cleavage-stage embryo. Furthermore, they provide novel insights into anterior morphogenesis.

Key words: dorsal axis determination, embryonic shield, morphogenetic cell movements, *gooseoid* homeobox gene, lithium teratogenesis, in situ hybridization

## INTRODUCTION

A fundamental process of animal development is dorsoventral specification. To understand this process, it is important to determine when the positional cues that signal dorsal first appear and function, and to determine their molecular identity (Davidson, 1990). In *Drosophila* development, these cues are established during oogenesis and dorsoventral polarity can be distinguished in the unfertilized egg (reviewed in St. Johnston and Nüsslein-Volhard, 1992). Dorsal specification also occurs quite early during the development of certain vertebrates. For example, amphibian dorsal (or embryonic) axis determination is initiated before the first cleavage, via the cortical rotation. In contrast, many vertebrate embryos do not appear to undergo cortical rotation, and specializations that morphologically mark the embryonic axis do not appear until gastrulation; thus, it is unclear when dorsal is first specified in these embryos. For example, the embryonic axis of the teleost embryo can be distinguished only at gastrulation, upon formation of the embryonic shield, which first identifies the dorsal side of the embryo. Shield formation generates an asymmetric gastrula from a morphologically symmetric blastula and a critical question of teleost axis formation is when do the cues that underlie the shield first arise and function.

Vertebrate axis specification is best understood in amphibians (reviewed in Gerhart et al., 1989). Fertilization,

which can occur anywhere within the animal hemisphere, triggers the cortical rotation, which introduces a novel asymmetry into the one-cell embryo, the vegetal dorsalizing (or Nieuwkoop) center. The region above this center, the grey crescent, corresponds to where the dorsal blastopore lip forms at gastrulation, and thus, the future position of the dorsal axis can be visualized in the one-cell embryo. Dorsal specification is a sequential process: the Nieuwkoop center induces overlying cells to develop as dorsal mesoderm, and these cells, in turn, populate the Spemann organizer. The organizer directly signals the production of the axis, which consists of both organizer and non-organizer cells.

Treatments that perturb axis specification in *Xenopus laevis* have demonstrated the importance of the cortical rotation and downstream signaling events. For example, UV irradiation of just-fertilized eggs, which blocks rotation, yields ventroposteriorized embryos (Scharf and Gerhart, 1983; Elinson and Rowning, 1988); conversely, exposure of cleavage-stage embryos to lithium ion yields radially symmetric dorsoanteriorized embryos (Bäckström, 1954; Kao and Elinson, 1986, 1988; Cooke and Smith, 1988). Significantly, lithium perturbs dorsal specification only when treatment occurs before the midblastula transition (Yamaguchi and Shinagawa, 1989); after this stage anterior defects are produced. These results are best understood in the context of the phosphoinositol (PI) signal transduction pathway (Busa and Gimlich, 1989; Maslanski et al., 1992;

reviewed in Berridge et al., 1989), as lithium inhibits inositol phosphatases to shut down the PI cycle. Thus, cortical rotation might produce the local inhibition of a signaling pathway that subsequently effects the local activation of organizer genes at the midblastula. Lithium, by globally inhibiting cell signaling, results in ectopic organizer gene expression, and thus, dorsoanteriorized development.

The identification of molecular asymmetries in the *Xenopus* blastula has begun to elucidate the molecular nature of the frog organizer. For example, the *gooseoid* (Blumberg et al., 1991; Cho et al., 1991), *XLIMI* (Taira et al., 1992), *XFkHI* (Dirksen and Jamrich, 1992) and *noggin* (Smith and Harland, 1992) genes are activated at, or shortly after, the midblastula transition and are locally expressed in dorsal blastopore lip cells. Significantly, lithium increases and radializes both *gooseoid* and *noggin* expression.

No symmetry breaking event equivalent to the cortical rotation, or region analogous to the grey crescent, can be distinguished in teleost development, which is best characterized for the zebrafish, *Brachydanio rerio* (Westerfield, 1989; Warga and Kimmel, 1990; Kimmel et al., 1990). While the zebrafish oocyte, like that of the frog, has an animal-vegetal axis, fertilization only occurs at the animal pole (Hart and Donavon, 1983). Following fertilization, non-yolky cytoplasm in the egg streams radially upward to segregate the blastodisc from the yolk cell. The blastodisc then undergoes several synchronous cleavages to produce, by the midblastula, a radially symmetric blastoderm atop the yolk cell. This stage is marked by the onset of zygotic transcription, asynchronous cell divisions and extensive cell rearrangements. Three cell movements, epiboly, involution and convergence-extension, reshape the radially symmetric midblastula into the bilaterally symmetric gastrula. In epiboly, the blastoderm thins and spreads radially downward to cover the yolk. The margin at which the migrating cells meet the yolk corresponds to the future blastopore, which will close near the vegetal pole. Gastrulation begins at 50% epiboly, when deep cells at the margin begin to involute underneath the blastoderm and migrate toward the animal pole. A thickened annulus, the germ ring, forms at this margin, and folds the blastoderm into the non-involuting epiblast and the involuted hypoblast, which give rise to the ectoderm, and the mesoderm and endoderm, respectively. Involution is initially symmetric, with no morphological sign of dorsal; however, soon after it begins, both epiblast and hypoblast cells converge toward one side of the embryo to produce a localized thickening of the germ ring in a 30° arc. This structure, which breaks the radial symmetry of the embryo, is the embryonic shield and marks dorsal. As gastrulation proceeds, the leading edge of the shield moves toward the animal pole, and the shield narrows and lengthens as converging cells intercalate, to produce the axis.

The embryonic shield is analogous to the amphibian dorsal blastopore lip, as the early shield can organize the formation of a complete secondary axis, consisting of both host and graft-derived cells, in a recipient embryo (Luther, 1935; Oppenheimer, 1936b, 1955; Eakin, 1939). Shield transplantation into an amphibian recipient also gives secondary axis formation (Oppenheimer, 1936c), suggesting that the amphibian and teleost organizers function via related molecules. While it is clear that the cues that under-

lie the frog organizer are generated at fertilization, it is unknown when the shield cues first appear and function. The fish blastula might truly be symmetric with the asymmetry that underlies axis formation first generated only at gastrulation; alternatively, an unidentified molecular asymmetry might be established in the cleavage-stage embryo and lead to the shield via a pathway of inductive interactions.

To distinguish between these models, we have asked whether dorsal axis specification can be experimentally perturbed, and whether a molecular asymmetry that predicts the position of the shield can be identified, in the pre-gastrula zebrafish. We show that brief lithium exposure of cleavage-stage embryos perturbs a pathway that underlies shield and dorsal axis formation: lithium produces embryos that exhibit radialized shields and hyper-dorsal development. Significantly, these effects are limited to exposure before the midblastula and later exposure produces anterior defects. We also present the molecular characterization of the zebrafish *gooseoid* homeobox gene and show that this gene is zygotically expressed at or just after the midblastula in a spatially localized domain of cells that give rise to the most anterior portion of the nascent shield and anterior axial hypoblast. Significantly, *gooseoid* expression is increased and radialized by early lithium treatment. Our results with lithium and *gooseoid* demonstrate that the zebrafish embryonic axis is specified by a pathway that functions in the cleavage-stage embryo.

## MATERIAL AND METHODS

### Embryos

Embryos from spawnings of zebrafish (Ekkwill Tropical Fish Breeders, Gibsonton, FL) were maintained at 28.5°C in ER water (60 mg per liter of Instant Ocean aquarium salt), and staged according to Kimmel (Westerfield, 1989; Warga and Kimmel, 1990), with developmental stages expressed as hours post-fertilization (h). For lithium treatment, embryos were exposed to 0.3 M LiCl in ER for 10 minutes and then washed with ER. These conditions were established using a range of LiCl concentrations and times of exposures. Also, identical results were obtained with chorionated and dechorionated embryos, so chorionated animals were used in all subsequent experiments. Embryos were anesthetized with tricaine (Westerfield, 1989) and photographed using an Olympus SZH stereomicroscope, or a Zeiss Axiophot microscope under DIC optics. For histochemical use, both dechorionated embryos and ovaries were fixed for 2 hours in MEMFA (0.1 M MOPS, pH 7.4, 2 mM EGTA, 1 mM MgSO<sub>4</sub> and 3.7% formaldehyde) and stored in methanol at -20°C.

### Cloning and characterization of zebrafish *gooseoid* cDNAs

The *Xenopus gooseoidA* cDNA coding sequence (Blumberg et al., 1991) was used to probe a gastrula-stage zebrafish ZapII cDNA library. Nylon filters were hybridized for 16 hours at 30°C in 6.25× SSC, 50% formamide, 25 mM Na<sub>2</sub>PO<sub>4</sub>, 1× Denhardt's, 250 µg/ml Torula RNA, 5% SDS and 5 mM EDTA, and washed for 2 hours in 2× SSC, 1% SDS at 37°C. 29 positives were obtained in 6×10<sup>5</sup> plaques. Eight independent clones were found to carry either a 1.3 kilobase (kb) insert (three clones; representative clone pZG10.3), or a 1.2 kb insert (five clones; representative clone pZG1.1). The complete DNA sequences of both clones

were determined using a transposon-mutagenesis/PCR sequencing procedure (Stachel and Dew-Jager, unpublished; GenBank/EMBL accession numbers L03394 and L03395, respectively). The last 801 residues encoding the C-terminal 136 residues of the zebrafish *goosecoid* protein and 3 noncoding region are identical between these two clones, while the N-terminal and 5 noncoding sequences are unrelated. The pZG10.3 insert, which encodes a longer predicted protein, was used in all subsequent experiments.

### RNA isolation and analysis

Total RNA was isolated from zebrafish embryos using a modified SDS/phenol protocol (R. Harland, personal communication). Staged embryos were frozen in liquid nitrogen and homogenized in a Dounce tissue grinder in 0.2 M LiCl, 50 mM Tris-HCl, pH 8.0, 10 mM EDTA and 1% SDS (1 ml per 100 embryos). The homogenate was added to an equal volume of water-saturated phenol and incubated at 65°C for 10 minutes. The aqueous phase was reextracted with phenol and twice extracted with chloroform/isoamyl-alcohol (24/1). Total RNA was precipitated by the addition of a one-quarter volume of 10 M LiCl at -20°C for 60 minutes and collected by centrifugation. The pellet was washed with 80% ethanol, dried, resuspended in DEPC-treated water and stored at -80°C. Embryos less than 10 h yielded about 300 ng/embryo of total RNA, while older embryos gave larger yields. For northern blot analysis, equal amounts of total RNA (assessed by A260 measurements and visualization of rRNA bands) were fractionated on a formaldehyde-agarose gel, transferred to a nylon membrane, and probed with the pZG10.3 cDNA insert.

### Whole-mount immunohistochemistry and in situ hybridization

*Xenopus* whole-mount immunohistochemistry (Patel et al., 1989; Hemmati-Brivanlou and Harland, 1989) and in situ hybridization (Harland, 1991) protocols were adapted to zebrafish embryos. Zebrafish embryos are fragile and both procedures were carried out using 'baskets' (made by cutting off the top and bottom of a 1.5 ml microfuge tube and melting 80-100 µm nylon netting onto the bottom). Embryos are placed into a basket and several baskets are supported by a rack in a staining dish, which is rocked (<80 revs/minute) on a platform shaker or in a water bath during the incubation and washing steps. For the hybridization step, each basket is placed into a small scintillation vial to which 0.5 ml of probe is added. For all antibody steps, the bottom of each basket is capped using the bottom half of a 2 ml cryogenic tube (Corning no. 25702) and >150 µl of diluted antibody is added.

For immunohistochemistry, fixed embryos were transferred to baskets, rehydrated over 15 minutes into PBT (PBS, 2 mg/ml BSA and 0.1% Triton X-100), and washed for 15 minutes in PBT and then 1 hour in PBT/10% heat-inactivated fetal calf serum (FCS; Gibco-BRL). The bottoms of the baskets were then capped and the embryos incubated overnight at 4°C in primary antibody in PBT/10% FCS. The embryos were subsequently washed 5×30 minutes in PBT, incubated for 2-3 hours at room temperature in goat anti-mouse IgG coupled to horseradish peroxidase (Biorad; diluted 1/200 in PBT/10% FCS). The embryos were then washed 5×30 minutes in PBT, transferred to a Corning Pyrex 9-well depression plate, incubated in 0.5 ml of the diaminobenzidine substrate (1 mg/ml; Polysciences) in PBT for 2 minutes and the chromogenic reactions (from 5 to 30 minutes) were catalyzed by 5 µl of 5% hydrogen peroxide. The reactions were stopped with two washes of PBS, and the embryos were dehydrated in methanol and cleared in BBA (2:1 benzyl benzoate/benzyl alcohol).

Four mouse monoclonal antibodies were used. MZ15 (Smith and Watt, 1985), which recognizes keratin sulphate, a primary component of the notochord sheath, was used at a 1/300 dilution of purified IgG resuspended at 1 mg/ml; F59 (Miller et al., 1985),

which recognizes both heart and skeletal muscle in the zebrafish embryo, was used at a 1/20 dilution of cell supernatant; 4D9 (Patel et al., 1989), which recognizes engrailed nucleoproteins found in several zebrafish embryonic cell types including the muscle pioneers and neural cells at the midbrain-hindbrain junction (Hatta et al., 1991), was used at a 1/1000 dilution of ascites; and Zn12 (Trevarrow et al., 1990), which recognizes the L2/HNK-1 epitope found on zebrafish neurons, was used at a 1/5000 dilution of purified IgG resuspended at 17 mg/ml.

Modifications to the in situ hybridization protocol of Harland (1991) included: use of baskets, limiting proteinase K digestion to 2 minutes, decreasing probe concentration to 0.5 µg/ml and increasing the high-stringency wash to 0.15× SSC, 0.3% CHAPS, 62°C. Also, the anti-digoxigenin antibody (Boehringer Mannheim) was preadsorbed to mixed zebrafish stages and used at a 1/2000 dilution in PBT/20% FCS; and the embryos were incubated in antibody for 4 hours at room temperature and washed overnight in PBT at 4°C. The alkaline phosphatase chromogenic reaction was carried out in capped baskets at 28.5°C for 9 hours with oocytes and premidblastula embryos, and for 3 hours with post-midblastula embryos (3.5 h and older). The stained embryos were fixed overnight in MEMFA/0.2% glutaraldehyde (Polysciences), dehydrated in ethanol and examined under dark-field illumination, or cleared in BBA and examined under bright-field illumination and DIC.

Sense and antisense digoxigenin-labeled RNA probes were synthesized with T3 and T7 RNA polymerase, respectively, and base-hydrolyzed to an average length of 200 bp, as described (Harland, 1991). The DNA template for these reactions was a PCR-generated fragment, using pZG10.3 and universal and reverse primers, which are distal to the T3 and T7 sites that border the pZG10.3 insert. Staining was only obtained in initial experiments with the antisense strand probe, confirming the hybridization and detection specificity.

## RESULTS

### Lithium perturbs two distinct developmental pathways in the zebrafish embryo

Brief exposure of cleavage-stage embryos to 0.3 M LiCl produces two defect classes, called bustled and radialized. Fig. 1 shows examples of these defects at 26 h. Considerable organogenesis has already occurred in control embryos (Fig. 1A): somitogenesis is complete, the initial circulation is evident and major elements of the central nervous system (CNS) have formed. Fig. 1B shows a bustled embryo. These embryos have a single axis whose posterior region is expanded in relative size and twisted into a bustle-like structure above the plane of the yolk. Cells observed throughout the length of the bustle have the vacuolated morphology and 'stack of pennies' arrangement of notochord cells. Bustled embryos often exhibit relatively normal dorsoanterior structures, including the eyes and ventricles of the CNS. In contrast, radialized embryos show no distinguishable unitary axis or differentiated anterior structures (Fig. 1C,D). They instead manifest several distinct regions of notochord-like cells that are separated by lobes of yolk and that often terminate in a mass of cellular material at either the animal or vegetal pole.

The bustled and radialized defects indicate that LiCl can severely perturb pattern formation. This effect is quite specific as embryos similarly exposed to other cations develop normally. Furthermore, essentially all embryos exposed to

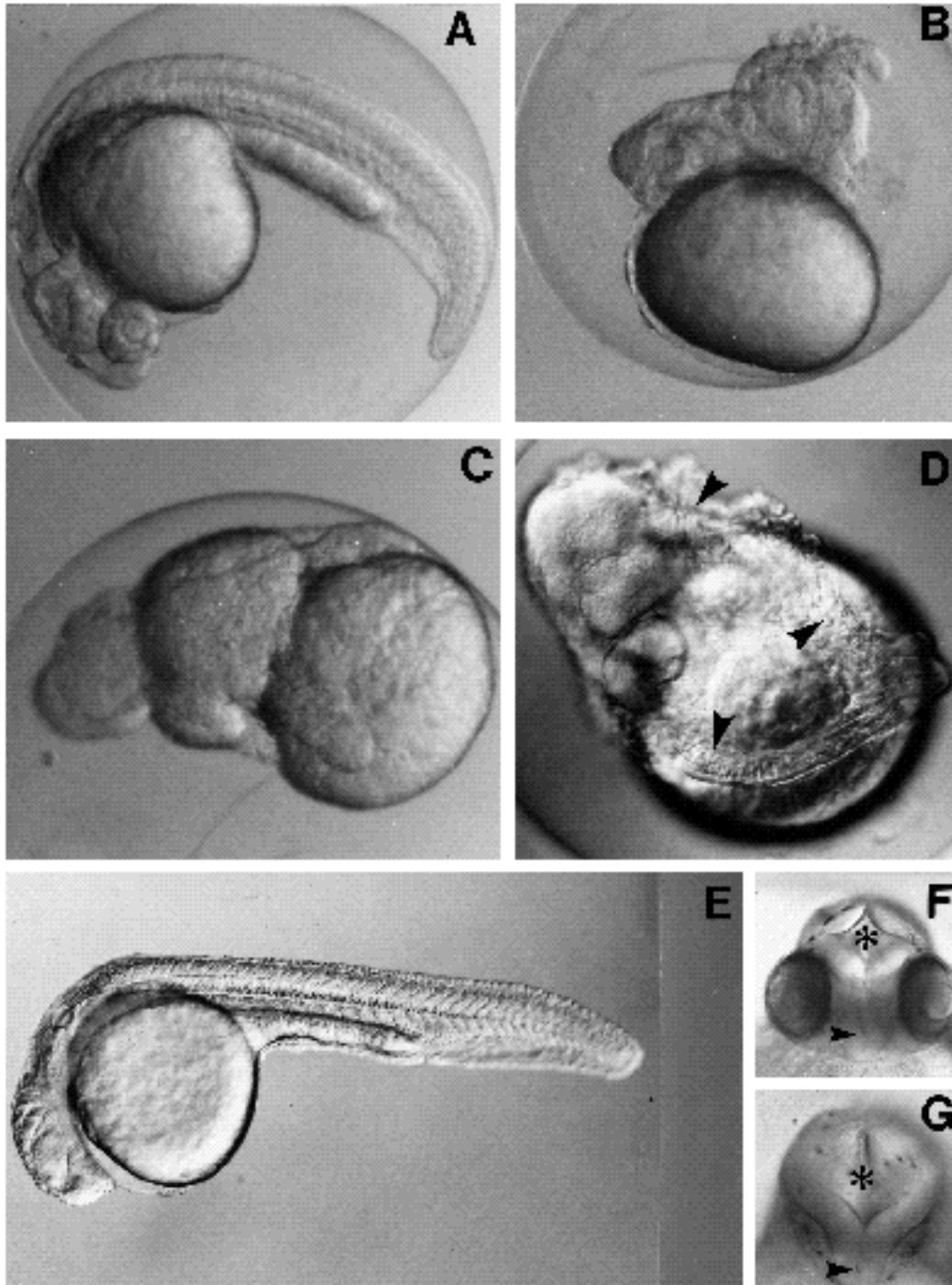


**Fig. 1.** LiCl produces three classes of defects in zebrafish embryos. Embryos were exposed to 0.3 M LiCl for 10 minutes at the 64-cell stage (2 h; B-D), and at the sphere stage (4 h; E and G), and photographed at 26 h (A-D) or 28 h (E-F). (A) Control embryo. (B) Bustled embryo. (C) Radialized embryo. (D) Radialized embryo. Arrowheads indicate distinct notochord-like structures. (E) Eye-defective embryo. (F) Dorsoanterior view of a control embryo CNS, with the first (\*) and third (arrowhead) ventricles indicated. (G) Equivalent view of an anophthalmic embryo.

lithium during early cleavage, which we call 'lithiumized' embryos, develop the bustled or radialized defects. These defects appear to belong to a single continuum and all the animals develop the radialized phenotype with longer times of exposure. More than 90% of these embryos can survive through early gastrulation, when they are still largely indistinguishable from the controls; however, with the onset of involution they become progressively misshapen, and many die during early somitogenesis (12 h), when they are often seen to burst within their chorions, and less than 50% survive to 24 h.

With later exposure, the embryos have a much higher survival rate and exhibit a third defect class, in which anterior development, and in particular eye development, is perturbed. These embryos, which have normal dorsal axes, lack eyes or have only very small eyes (Fig. 1E), and many also display more extensive anterior deficiencies. Lithium retards *Xenopus* gastrulation movements to result in incomplete involution and the corresponding incomplete induction of anterior structures (Regan and Steinhardt, 1988; Stewart and Gerhart, 1990). Retarded gastrulation cannot account for the embryos here that only exhibit eye deficits,

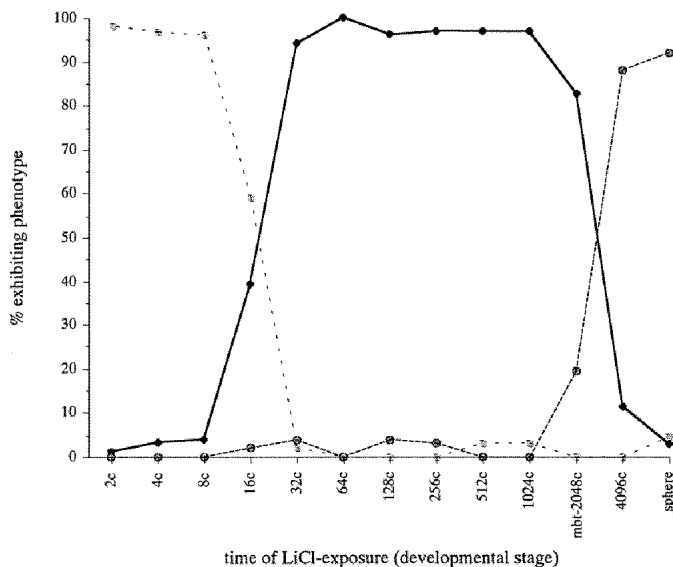


**Fig. 2.** Developmental phenotype versus time of LiCl exposure. Groups of at least 100 staged embryos were exposed to 0.3 M LiCl for 10 minutes at the indicated times, from the 2-cell stage to the late blastula, and allowed to develop at 28.5°C. Phenotypes were scored at 26 h and the % phenotype was calculated with respect to the total number of survivors within each group. The results were averaged from two separate experiments and represent more than 3000 embryos. Three categories of phenotypes were scored: normal development (—■—); radialized and bustled defects (---◆---); and eye-defects and anterior deficiencies (---○---). The midblastula transition (mbt) occurs around cleavage 11. Note that exposure after the late-blastula is generally lethal.

as CNS structures anterior to the eyes are present in these animals: while the optic vesicles bud off from the third ventricle, the first through third ventricles are clearly present in the anophthalmic embryo of Fig. 1G (compare with the Fig. 1F control embryo).

Fig. 2 shows that essentially all embryos treated between the 4th and the 11th cleavages exhibit bustled and radialized defects, and between the 11th cleavage through early gastrulation exhibit eye or head defects. Thus, LiCl teratogenesis undergoes two transitions. The first transition occurs at the 16-cell stage, when lithium sensitivity is first observed, to suggest that before this stage lithium cannot gain entry into the embryo, or the biochemical pathway perturbed by lithium is not yet present or is sequestered. The second transition occurs at the 2000-cell midblastula stage, when lithium no longer produces the bustled and radialized defects. This transition is not due to a loss of penetrance, as increased times of late LiCl exposure, which produce high rates of lethality, still do not effect the bustled or radialized defects. Lithium teratogenesis in *Xenopus* similarly shows these two transitions (Yamaguchi and Shinagawa, 1989). The results of Fig. 2 further indicate that lithium disrupts two distinct pathways, to produce severe pattern defects and anterior defects, respectively.

### Hyper embryonic shield development in lithiumized embryos

The normal shield at 6 h appears as a local thickening and

anterior swelling of the germ ring (Fig. 3A), which, due to cell convergence, contains more cells than adjacent regions. Similar shield morphologies are not seen in 6 h lithiumized gastrulae, which instead exhibit overly broad (Fig. 3B) and/or supernumerary (Fig. 3C) thickenings along their germ rings, with a limit form in which the shield looks fully radialized (Fig. 3D). In contrast, shields appear normal in embryos treated with lithium after the 2000-cell stage. Thus, by morphological criteria, excess shield material is generated in gastrula-stage embryos exposed to LiCl before the midblastula stage.

### Hyper convergence-extension in lithiumized embryos

If lithium perturbs axis specification and produces excess organizer material, then both morphogenetic cell movements and the differentiation of specific tissues should be aberrant in lithiumized embryos. For example, since the shield organizes and is the focus of convergence-extension movements, these embryos should undergo excessive and radialized convergence-extension. Control 12.5 h embryos contain 7 to 8 pairs of somites bilaterally arranged over the center of the yolk and separated by the notochord (Fig. 3E); also, as convergence-extension within the tailbud has so far been limited, it has not yet begun to extend away from the yolk. In contrast, lithiumized 12.5 h embryos typically have a large cylindrical extension off their posterior surface, with the blastopore located at its terminus. These forms suggest that massive posteriorwards convergence-extension movements are occurring. Gastrulae with single broad shields produce segmented extensions (Fig. 3F), and develop the bustled phenotype; gastrulae with supernumerary and/or radialized shields yield extensions lacking obvious organization (Fig. 3G), and develop the radialized phenotype. Morphogenetic movements in these extreme forms might occur circumferentially towards the interior to produce a radially symmetric extension. Similar movements more anteriorwards could bisect the yolk into separate regions, as is seen in 26 h radialized embryos (Fig. 1C,D).

A second perturbation often exhibited by 12.5 h lithiumized embryos is the extrusion through the blastopore of part of the yolk, which then frequently becomes covered over by posteriorly extending tissue (Fig. 3H). These forms suggest that early lithium treatment can result in the inhibition of epiboly, with the blastopore failing to reach the vegetal pole and prematurely closing onto the yolk. These effects could be due to the radial buildup of excess cells undergoing convergence-extension movements within the germ ring.

### Hyper-dorsal development in lithiumized embryos

The teleost organizer, which is localized to the embryonic shield, is thought to divide the hypoblast into axial and paraxial components. Involved cells near the shield are recruited to converge into the dorsal midline and form the axial lineage. These cells populate the chordamesoderm, which gives rise anteriorwards to the prechordal plate and posteriorwards to the notochord, and also probably the endoderm. In contrast, the more lateral hypoblast populates the paraxial lineage, which gives rise anteriorwards to the

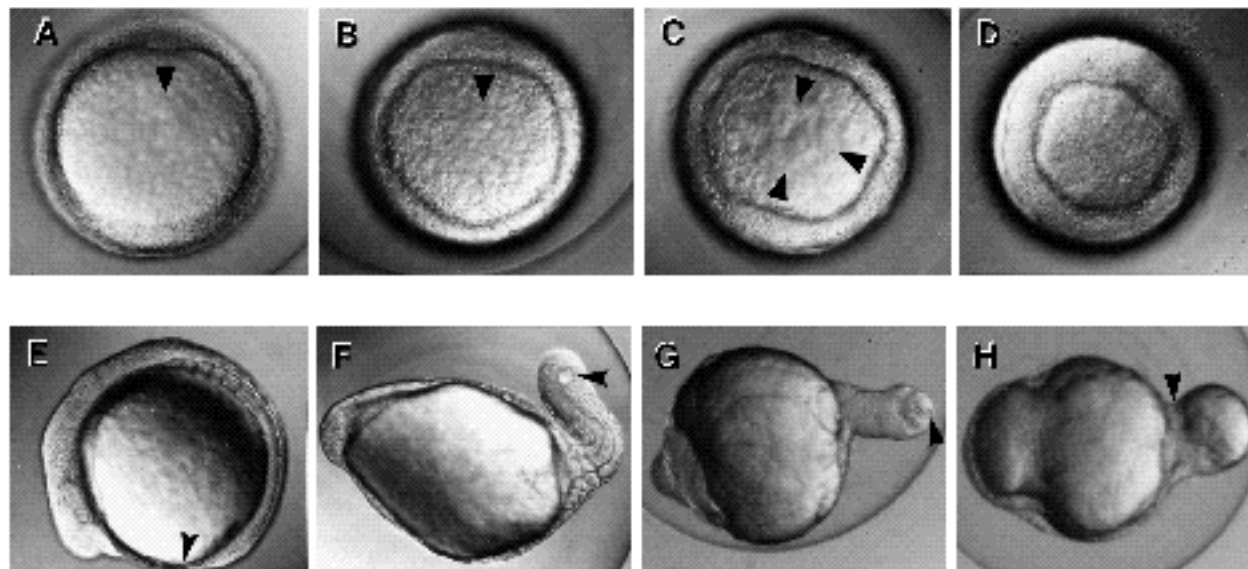


**Fig. 3.** Early lithium exposure leads to excess shield formation and aberrant morphogenesis. (A-D) Animal pole views of 6 h embryos. Arrowheads mark the location and presumptive direction of migration of regions of the germ ring having embryonic shield morphology. (A) Control embryo. The shield appears as an anterior thickening of the germ ring and occupies a  $30^\circ$  arc. (B) Lithiumized embryo, broadened shield. A single thickening at the germ ring subtends a  $90^\circ$  arc. (C) Lithiumized embryo, supernumerary shields. (D) Lithiumized embryo, radialized shield. (E-H) Lateral views of 12.5 h embryos. Anterior is to the left in each panel. The blastopore in each embryo is indicated by an arrowhead. (E) Control embryo. Seven somites have formed, and the tailbud, which is just caudal of the blastopore, has not yet extended off the yolk. (F) Lithiumized embryo. A large mass of segmented tissue extends posteriorly, with the blastopore located at its terminus. (G) Lithiumized embryo. The large posterior extension is unsegmented. (H) Lithiumized embryo. The blastopore has closed onto and bisected the yolk, and the extruded portion of the yolk is partially covered by posteriorly extending cellular material.

head mesoderm and posteriorwards to the prospective somite muscle and the lateral mesoderm. This division of the hypoblast predicts that embryos with excess organizer should differentiate a surplus of axial, and a deficit of paraxial, mesoderm. Fig. 4 shows that lithiumized embryos manifest such hyper-dorsal development.

Axial mesoderm was assessed with MZ15, an antibody that stains the otic capsule and the notochord sheath, which in control embryos appears as a straight rod that begins just behind the ears and extends caudally to the end of the tail (Fig. 4A). In contrast, the bustled notochord is highly twisted (Fig. 4B), and appears to be relatively enlarged. More strikingly, radialized embryos exhibit many distinct notochords, which often spread over all sides of the embryos and constitute much of their cellular material. The radialized notochords can be quite extended, twisted and branched, and frequently terminate in a mass of stained tissue located in some specimens around the blastopore (Fig. 4C), and in others around the animal pole. These latter forms possibly reflect the extent that epiboly has gone to completion (see Fig. 9). Also, small independent segments of notochord are scattered throughout many radialized embryos, suggesting that notochord induction has occurred at several separate sites (Fig. 4D). Thus, early lithium exposure leads to the differentiation of excess notochord and supernumerary embryonic axes.

Paraxial mesoderm was assessed with F59, an antibody that stains the heart and the somites, which in control embryos appear as two bands of tissue, separated by the notochord and spinal cord, down the length of the trunk

(Fig. 4E). The rostral boundaries of this tissue and the notochord are roughly coincident. Lithiumized embryos have a deficit of skeletal muscle. For example, the somite muscle in bustled embryos fails to extend to the anterior end of the notochord and is reduced in relative amount (Fig. 4F), and is seen at higher magnification to have aberrant myofibril organization. More strikingly, the amount of somite muscle in radialized embryos is severely reduced and many separate regions of staining are often observed (Fig. 4G,H). The embryo in Fig. 4H is sprinkled circumferentially with small patches of muscle, again suggesting that radialized embryos can have multiple embryonic axes.

Since induction and formation of the CNS occurs in conjunction with the dorsal axis, embryos with multiple axes should exhibit multiple sites of neurulation. Lithiumized embryos exhibit such supernumerary neural development. Using 4D9, which stains neural cells at the mesencephalon-rhombencephalon border (control embryo, Fig. 4I), the lithiumized embryos in Fig. 4J,K have several distinct foci of neural staining, while a complete ring of staining is observed for the embryo in Fig. 4L. Similar results were also obtained with the neural specific ZN-12 antibody, and with several neural specific genes. Thus, lithium can lead to supernumerary sites of neural induction, as well as radialized induction around the entire embryo.

#### **Molecular characterization of zebrafish *gooseoid***

The preceding results show that the zebrafish dorsal axis is specified by a pathway that functions at least 2.5 hours prior to the appearance of the shield. Since a critical component

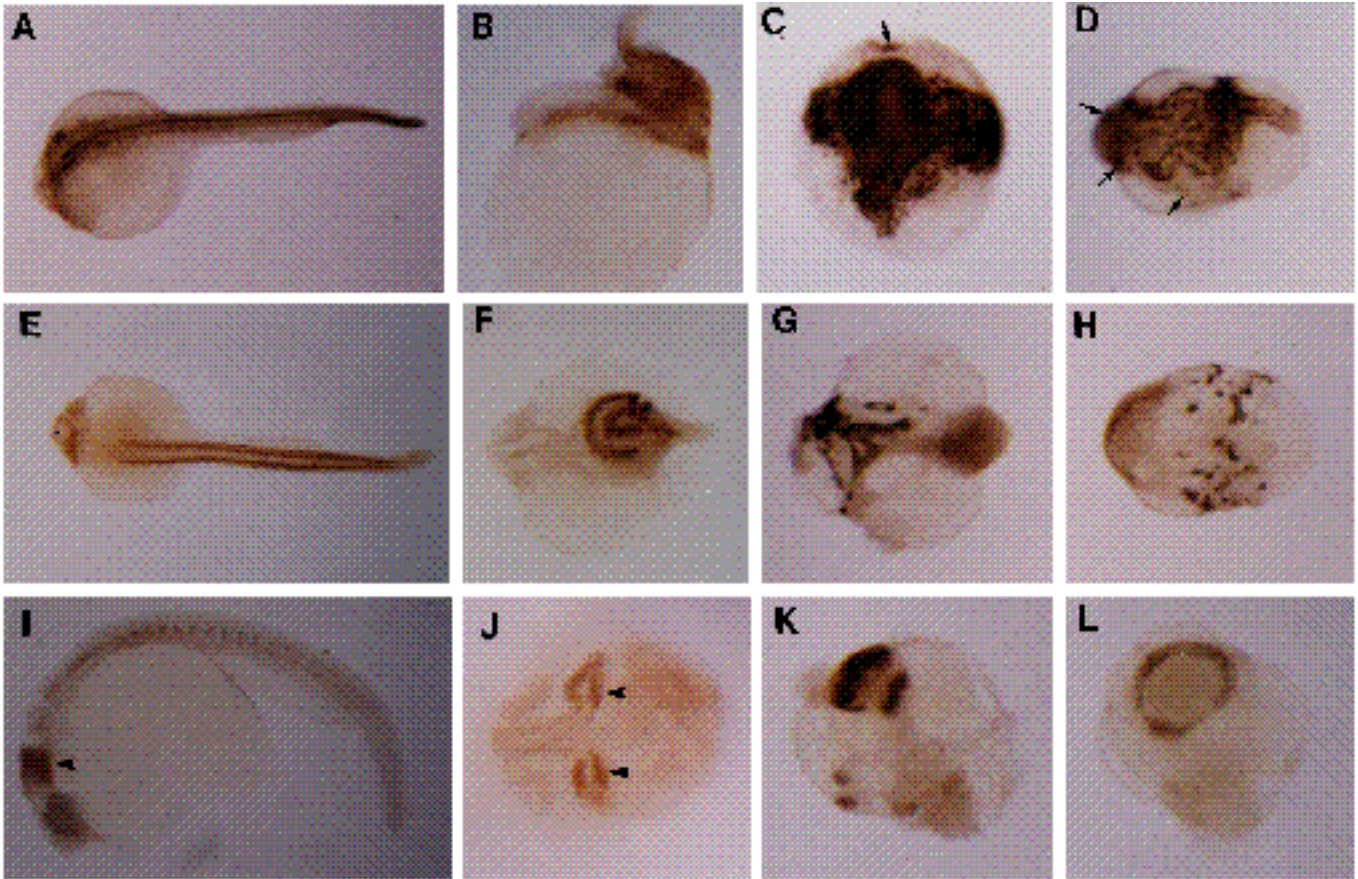


**Fig. 4.** Immunohistochemical analysis of hyper-dorsal development in 26-28 h lithiumized embryos. Anterior is to the left in all panels for which orientation can be determined. (A-D) Analysis of notochord differentiation with MZ15. (A) Control embryo, dorsal view. The anterior end of the notochord sheath is just behind the ears. (B) Bustled embryo, lateral view. The notochord is highly twisted and its anterior end is much more posteriorwards than for the control. (C) Radialized embryo, vegetal-pole view. Several distinct and twisted notochords radiate anteriorwards from a large mass of stained tissue that surrounds the blastopore, which has prematurely closed onto the yolk. (D) Radialized embryo, indeterminate orientation. Arrows in C and D indicate distinct patches of notochord tissue. (E-H) Analysis of skeletal muscle differentiation with F59. (E) Control embryo, dorsal view. Heart staining is to the left, anterior to the ears. The somite muscle appears as two lateral bands down the length of the trunk. (F) Bustled embryo, dorsal view. No heart staining is seen. The skeletal staining appears as two twisted lateral bands. (G) Radialized embryo, indeterminate orientation. The muscle staining, which is greatly reduced in relative amount, is highly disorganized. (H) Radialized embryo, indeterminate orientation. Several small patches of muscle tissue occur around the circumference of this specimen. (I-L) Analysis of neural engrailed expression with 4D9. (I) Control embryo, lateral view. Neural engrailed staining describes a band of cells at the midbrain-hindbrain junction, and muscle engrailed staining marks muscle pioneer cells located bilaterally within each somite. (J) Bustled embryo, dorsal view. A single anterior axis bifurcates at the level of the diencephalon to produce two foci of neural engrailed expression. Arrows in I and J indicate neural staining. (K) Radialized embryo, indeterminate orientation. Multiple sites of neural engrailed staining are observed. (L) Radialized embryo. Neural staining describes a complete band around the embryo, indicating that neural induction has occurred radially versus linearly. Such staining can coincide with the position of the blastopore in embryos that fail to complete epiboly. Note that radialized engrailed staining is similarly observed in lithiumized *Xenopus* embryos (Hemmati-Brivanlou and Harland, 1989).

of this pathway is lithium sensitive, and this sensitivity is limited to the period before the midblastula, a molecular transition must occur that converts dorsal axis information from a lithium-sensitive form in the cleavage-stage embryo into a lithium-insensitive form in the blastula. This transition could correspond to the localized activation of one or more genes that underlie shield formation. Since such genes might later be expressed in shield cells, the identification and characterization of a shield marker could lead to the elucidation of an 'organizer field'. To this end, we isolated and characterized zebrafish *goosecoid* cDNAs.

Fig. 5 shows the predicted protein sequence encoded by

the zebrafish *goosecoid* gene aligned against the predicted protein sequences of the *Xenopus* and mouse genes. Two domains that roughly divide the protein in half, can be distinguished. The C-terminal region, which contains the homeodomain, is highly conserved, and the homeodomains are identical, except for a conservative Lys to Arg substitution. The conservation decreases in the N-terminal region and several gaps are required to maintain the alignments. Comparing the zebrafish to the *Xenopus* sequence gives an overall identity of 78%, not including conservative changes. The identity from the aminoterminal through residue 115 is 64%, and from residue 116 through the carboxyterminus

```

Z  --AG-----s---g---s---DSV-L  hrNA-VV-Sn- tE---tAAGdfngl-S  htgPp-- 58
X  --sG-----N---A---R---eSL-L  PqNg-1l-Ss- GE---GpA  D-SgFYnwtV-- 55
M  --As-----N---A---R---DaV-pvapsaaa-VV-pa-hGd---GAgCgtssD-gaFYprPV-- 64
con MPagMFSIDnILAARPrCKdsvLl.....naPvvFs.L.geSLYgaag....dYs.fy..pvAP

Z  nLQs-NG -i---N-Y-----V- g-t--A---iPt--s--- -ciT--DsA----I 114
X  tsaLQg-NGS-L---N-Y-----l- t-v--s---Vga--t---SCV-saT--DGA---I 116
M  ggaglpaa-gsS-L---s-f---s---V-aa-V--A---Vfp--a---SCV-tpp--eGp---v 128
con .....lq.VngsRlGYnNyYgQLHvQ...FvGPaCCGAvp.LG.QQCscvP...tGYdgaGSVLI

Z  S-----ms----- 178
X  p-----LP----- 180
M  S-----LP----- 172
con sPVPHQMIpYMNVTLSRTELQLLNQLHCRKRRTIFTFDEQLEALENLFOETKYPDVCTREQ

Z  ---K-----sQ----- -t-tts- -i-EG---v--- 240
X  ---r-----AQ----- -S-nSa--Rd-ga---L--- 243
M  ---K-----Ae----- -t-S-aSp--Re-EG---L--- 256
con LARKVHLREEKVEVWFKNRRRAKWRQRSSSESESENaqKWNK.SsK.s.Ekr.EegKSDLDSDS
    
```

The 60 amino acid homeodomain is underlined. Note that the zebrafish DNA sequences immediately distal of the predicted amino and carboxytermini are unrelated to the corresponding *Xenopus* and mouse DNA sequences.

**Fig. 5.** Alignment of the zebrafish, *Xenopus* and mouse *gooseoid* proteins. The zebrafish protein sequence (Z) was predicted from the pZG10.3 cDNA sequence, and the *Xenopus* (X; Cho et al, 1991) and mouse (M; Blum et al., 1992) sequences are from the EMBL/GenBank database (accession numbers M81481 and M85271, respectively). For the aligned sequences, dashes indicate residues that are identical in all three sequences, and spaces indicate introduced gaps. For the consensus sequence (cons), upper case residues are identical in all three sequences, lower case residues are identical in two of the three sequences, and residues indicated as ( ) are different in all three sequences.

is 90%. Since tetrapods and fish diverged about 400 million years ago (Carroll, 1988), this degree of conservation is striking.

**Maternal and zygotic *gooseoid* transcription**

Fig. 6 shows the developmental expression of zebrafish *gooseoid*. Three transcripts are observed: a minor 2.75 kb transcript, and major 1.4 kb and 1.3 kb transcripts. With longer exposure, a 2.4 kb and a 1.7 kb transcript are also seen. The relative amount of each of the five transcript species, with respect to the other species, appears roughly constant in all stages assessed for expression.

*gooseoid* is maternally expressed and the amount of the maternal transcripts is much greater in the oocyte versus the zygote. An increase in transcript levels is first observed at 4 h, which closely follows the midblastula transition and the start of epiboly; we have not examined time points between 3 h and 4 h, to determine when *gooseoid* is activated. The zygotic transcripts are maintained at roughly constant levels up through 10 h, the start of somitogenesis, and then decline such that they are no longer detected by 15 h. Also, transcripts are observed in adult females but not males. Thus, *gooseoid* expression is limited to oogenesis and early embryogenesis.

**Zygotic *gooseoid* transcripts define a preshield domain**

The spatial localization of maternal and zygotic *gooseoid* transcripts was assessed using whole-mount in situ hybridization at 1 hour intervals from oogenesis through neurogenesis (15 h). Prior to the midblastula, *gooseoid* transcripts are uniformly distributed in both oocytes and embryos: positive staining is observed throughout immature and mature oocytes but not in the associated follicle cells (not shown). Following fertilization, hybridization is limited to the blastoderm and all the blastomeres up through 3.5 h of development appear equally stained. Thus, maternal *gooseoid* transcripts are not spatially localized in the oocyte or embryo. The functional significance of these transcripts is unclear, especially as *Xenopus gooseoid* is not maternally expressed (Cho et al., 1991).

We first detect localized *gooseoid* hybridization soon after the midblastula transition, at 4 h (Fig. 7A). Because this stage coincides with the initial increase in *gooseoid* transcript levels and closely follows the onset of transcription, the localized hybridization corresponds to zygotic transcripts. This hybridization first appears as a faint patch of stained cells that subtends an arc of 40° to 45° just within the blastoderm margin. Thus, molecular asymmetry exists in the zebrafish embryo at least 2 hours prior to the appear-

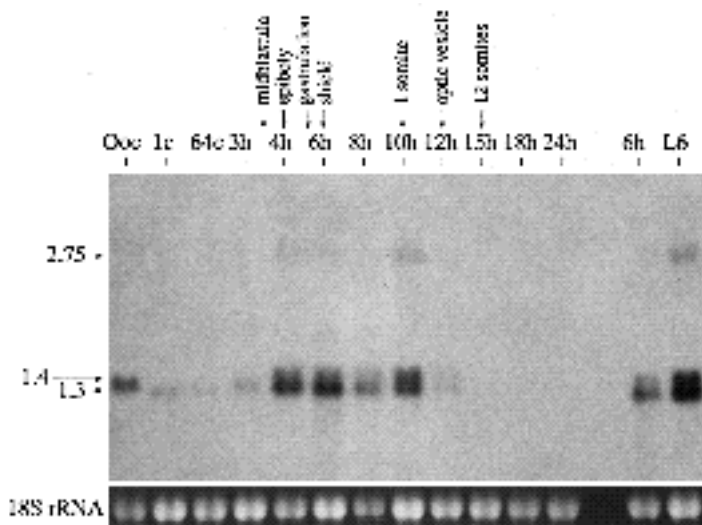


**Fig. 6.** Northern blot analysis of *gooseoid* expression in oocytes, staged embryos and LiCl-treated embryos. 4 µg samples of total RNA from zebrafish oocytes (mixed stages) and embryos of the indicated stages were fractionated on a 1% formaldehyde-agarose gel, transferred to a nylon membrane and probed with the entire 1.3 kb pZG10.3 cDNA insert. RNA concentrations were estimated from A260 measurements, and the 18S rRNA band intensities are shown at the bottom. Note that roughly three-fold less RNA was loaded in the 8 hour versus the adjacent lanes. Developmental stages correspond to hours post-fertilization except Ooc, 1c, 64c, and L6, which respectively correspond to oocytes (mixed stages), 1-cell embryos (15-30 minutes postfertilization), 64-cell embryos (2 hours postfertilization) and 6 h lithiumized embryos. Developmental landmarks and the sizes of the three major *gooseoid* transcripts are indicated at the top and left of the figure. Transcript sizes were calculated from the mobilities of RNA standards.

ance of the embryonic shield, the primary morphological asymmetry.

Soon after it is first detected, the intensity and extent of the localized hybridization, which is highest near the margin, increases to describe a 60° to 90° sector (Fig. 7B). The extent of this staining with respect to the animal pole varies from embryo to embryo, and is sporadic within the sector, and both deep and superficial cells initially express *gooseoid*. Two cell types populate the teleost blastoderm: the superficial enveloping layer cells, and the deep cells, which give rise to the embryo (Kimmel et al., 1990). At 5 h *gooseoid* hybridization is completely restricted to deep cells along the margin of the blastoderm within a 90° arc (Fig. 7C), and most cells within this domain are stained.

By 6 h, when the shield appears, the hybridization narrows to a 30°-40° arc that is limited by the boundaries of the nascent shield. This narrowing is likely due to the convergence of the most lateral *gooseoid* cells toward the center of the expression domain. Lateral observation of 6 h embryos indicates that the hybridization is localized to cells beneath the germ ring which appear to coincide with the leading edge of migration (not shown). Thus, *gooseoid* labels the cells that first involute and medially converge to generate the shield. Furthermore, as these cells are most likely descended from the *gooseoid*-expressing cells of the midblastula, *gooseoid* appears to mark an organizer-field that predicts the embryonic axis.

#### ***gooseoid* marks the anterior shield and axial hypoblast**

Following the onset of gastrulation, *gooseoid* expression is restricted to the hypoblast. At 8 h, the hybridization describes a medial-strip whose anterior border marks the leading edge of the shield as it narrows and extends toward the animal pole (Fig. 7E). This strip occupies a deep position in the embryo, beneath the epiblast, and over time its posterior limit narrows to a point. Significantly, staining is no longer observed at the margin by 8 h, and thus *gooseoid* only marks the anterior shield, which forms during early gastrulation. In contrast, the posterior shield continues to be built throughout gastrulation by the dorsal convergence of newly involuted cells near the margin. That *gooseoid* is restricted to the anterior shield suggests that most if not all of the *gooseoid* cells in the gastrula are descended from the cells that first express *gooseoid* in the blastula.

The leading edge of *gooseoid* hybridization reaches the animal pole between 8 h and 9 h, and by 10 h manifests the pattern seen in Fig. 7F. This pattern consists of the posterior V-shaped medial-strip and the anterior rostral-crescent, which coincides with the rostral and anterolateral boundaries of the embryo. The most intense hybridization occurs within the medial portion of the crescent and describes a broad swelling that appears to be partially folded back on itself at its dorsoposterior edge. Stained cells along the lateral edges of this structure are arranged into wing-like extensions just below the surface of the embryo, and *gooseoid* expression within these 'wings' appears to be somewhat variable and sporadic. Significantly, while the medial-strip cells are quite ventral to the crescent cells, the hybridization is completely contiguous

between the two patterns, which are joined through the medial swelling of the crescent (see Fig. 10). This continuity suggests the two patterns belong to a single domain of *gooseoid* expression.

By 12 h, staining is largely absent from the midline and confined to cells scattered along the rostral and lateral borders of the embryo (Fig. 7G). As hybridization can no longer be detected after 13 h, the functional role of *gooseoid* is probably limited to early embryogenesis. Up through 9 h, the *gooseoid* cells belong to the axial hypoblast. While the lateral staining at 10 h and later could be assigned to the paraxial hypoblast based on position, we think it also corresponds to axial cells that have been laterally displaced. Thus, *gooseoid* expression is likely restricted to the anterior axial hypoblast. Since this expression disappears during early organogenesis, we cannot assign the fates of the *gooseoid*-expressing cells. Based on lineage studies (Kimmel et al., 1990; T. Schilling and C. Kimmel, personal communication), they should populate those tissues derived from the fish anterior axial hypoblast: the 'polster' (thought to be equivalent to the amphibian prechordal plate), the pharyngeal endoderm and the hatching gland. These cells should not populate head mesoderm, which is derived from paraxial tissue. Also, *gooseoid* is not expressed in prenotochord cells, since *gooseoid* and a probe that marks prospective notochord (R. Riggleman, personal communication) stain entirely non-overlapping domains in 8 h and 10 h embryos (not shown). In contrast, *Xenopus* notochord cells are reported to express *gooseoid* (Cho et al., 1991).

#### **Elevated and radialized *gooseoid* expression in lithiumized embryos**

By morphological and developmental criteria, lithiumized embryos develop excess organizer tissue and expanded and radialized shields. Thus, we would predict that, if *gooseoid* marks an organizer field that underlies the shield, then its expression should be elevated and broadened in these embryos. The right side of Fig. 6 shows that *gooseoid* transcripts are elevated in lithiumized versus control 6 h embryos. This increased expression coincides with *gooseoid* activation, and its initial distribution is highly aberrant: while lithiumized and control embryos exhibit indistinguishable patterns of hybridization up through the midblastula (not shown); at 4 h, when faint localized staining is first seen in control embryos, substantial staining occurs throughout most or all of the blastomeres in lithiumized embryos (compare Fig. 8A with Fig. 7A,B). Thus, early lithium treatment results in global activation of *gooseoid*. Following this activation, *gooseoid* expression becomes secondarily localized to the margin in lithiumized embryos. For example, although significant staining still occurs throughout the 5 h blastoderm (Fig. 8B), most of the hybridization is concentrated around the margin and, by 6 h, the staining is completely restricted to the margin (Fig. 8C,D).

The spatial distribution of *gooseoid* expression in 5 h and 6 h embryos molecularly demonstrates that premidblastula lithium exposure results in the expansion and radialization of the organizer field. For example, while the marginal staining describes a 90° arc in 5 h control embryos,

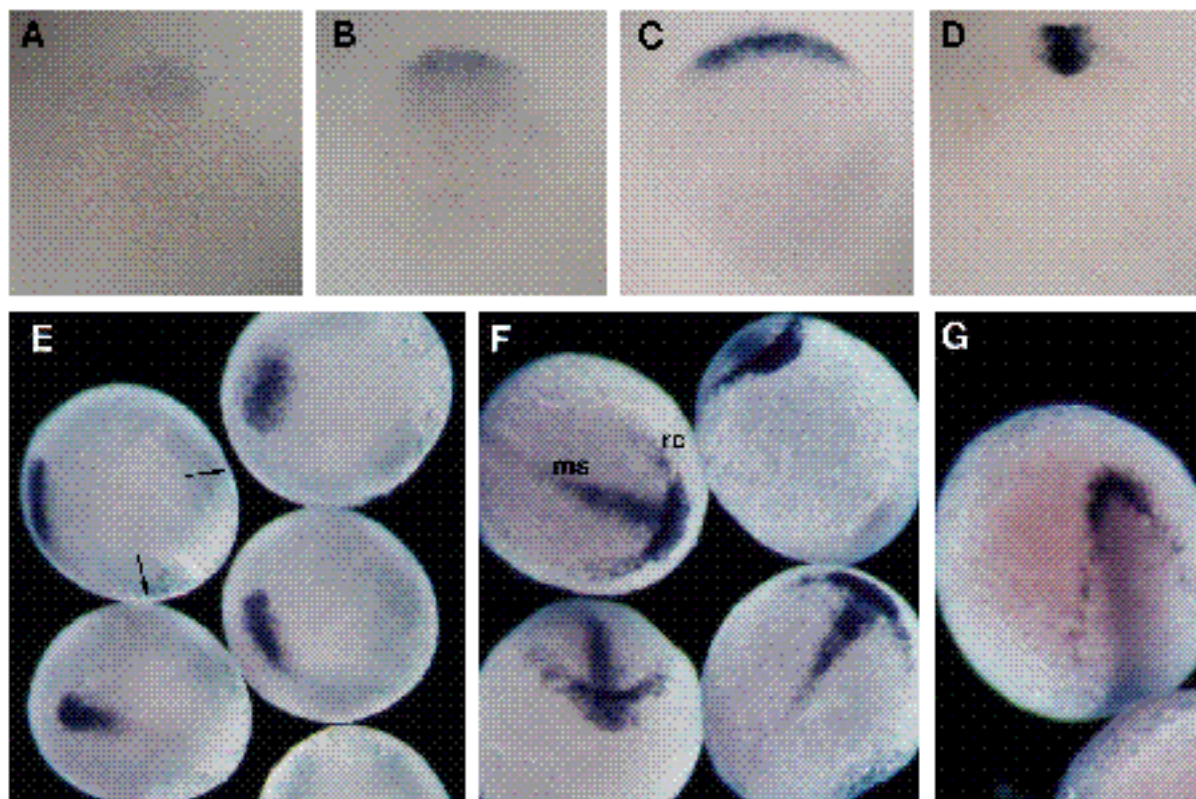


**Fig. 7.** Spatial localization of *goosecoid* transcripts during embryogenesis. Developmental times are  $\pm$  15 minutes. The blue staining corresponds to *goosecoid* hybridization. For A-D, the yolks were removed and the blastoderms were photographed in bright field. (A) Animal pole view of 'early' 4 h embryo. Expression is limited to a faint patch of cells. (B) Animal pole view of 'late' 4 h embryo. The expression domain has expanded to describe a  $90^\circ$  sector. (C) Animal pole view of 5 h embryo with staining limited to cells along the margin. Most cells within the expression domain exhibit staining by this stage. (D) Vegetal pole view of 6 h embryo. Hybridization is restricted to involuted cells within the shield. For E-G, the yolks were left intact, and the embryos were photographed in dark field. (E) Lateral and dorsal views of 8 h embryos. The arrows in the upper left embryo indicate the blastopore at the germ-ring/yolk margin. (F) Anterior and dorsal views of 10 h embryos. The blastopore has closed just ventral to the vegetal pole and the anterior edge of the hybridization is at the animal pole. The medial-strip (ms) and rostral crescent (rc) patterns are indicated in the upper left embryo. The rostral crescent is seen to occupy a position superficial to that of the medial-strip in the top embryo. Staining is sporadic in the lateral regions of the wing-like extensions of the rostral crescent. (G) Dorsal view of 12 h embryo, with sporadic staining along its anterolateral margins. Medial staining is no longer seen.

the entire circumference of the margin is stained in most 5 h lithiumized embryos. Furthermore, while the domain of *goosecoid* expression in 6 h controls encompasses a  $30^\circ$  arc at the germ ring, 6 h lithiumized embryos exhibit greatly broadened arcs of expression (Fig. 8D), and completely radialized expression (Fig. 8C). These patterns, which correspond to the aberrant shield morphologies shown in Fig. 3, further demonstrate that lithium leads to broadened and radialized embryonic shields.

Lithiumized 8 h embryos exhibit a ring of *goosecoid* staining above the margin, demonstrating that *goosecoid* cells belong to the migrating hypoblast (Fig. 8E). By 10 h, the staining is much further anteriorwards and the normal rostral-crescent and medial-strip patterns are not observed (Fig. 8F) and, by 12 h, the hybridization describes a large circular cap centered at the animal pole. These results show that although the processes that underlie the rostral-crescent and medial-strip patterns are disrupted in radialized embryos, involution and hypoblast migration movements still occur.

Significant animal pole staining is observed at 14 h (Fig. 8G) and, by 18 h, hybridization is no longer detected; thus, as for control embryos, *goosecoid* turns off during organogenesis. That staining is still seen several hours after it has disappeared in the controls could reflect that the increased levels of transcripts take longer to clear, or that transcription is prolonged, in lithiumized embryos. Also, we suspect that the increased *goosecoid* expression is related to the high mortality of lithiumized embryos, since early retinoic acid treatment, which down-regulates *goosecoid* expression (not shown), significantly increases the survival of lithiumized embryos to 24 h.

#### Late-lithium treatment disrupts lateral *goosecoid* patterning

Analysis of *goosecoid* expression also gives insight into the eye defects and anterior truncations seen in 'late-lithium' (post-midblastula exposure) embryos. Up through 8 h, the levels and spatial distribution of *goosecoid* transcripts in these embryos are indistinguishable from control embryos.

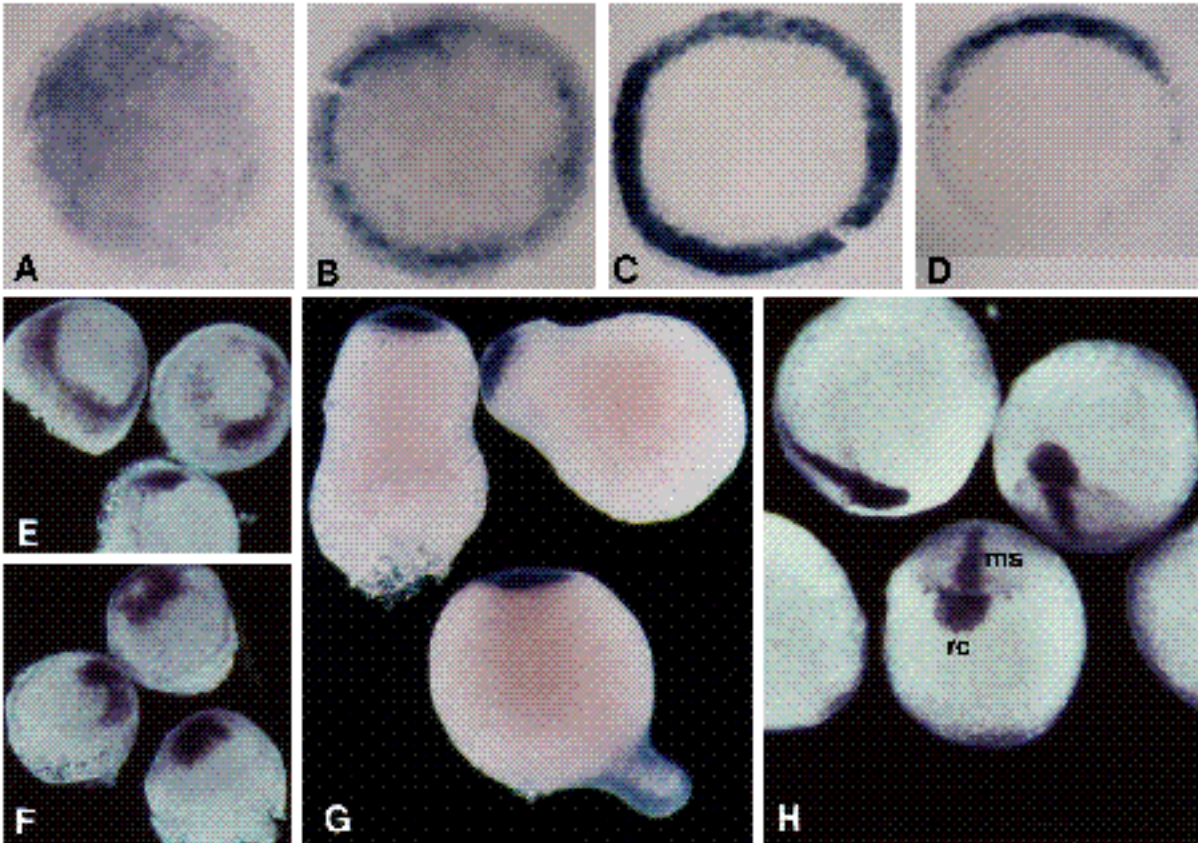


**Fig. 8.** Spatial localization of *goosecoïd* transcripts in lithiumized embryos. Stages are  $\pm$  15 minutes. Embryos in A-G and in H were exposed to 0.3 M LiCl for 10 minutes at 2 h and 4 h, respectively. For A-D, the yolks were removed and the blastoderms were photographed in bright field. (A) Animal pole view of a 4 h embryo. Staining is observed throughout the blastoderm; this staining is typically slightly more intense in a portion of the blastoderm. (B) Animal pole view of a 5 h embryo. While significant hybridization still occurs throughout the blastoderm, the staining is largely concentrated around the margin. (C) Animal pole view of 6 h embryo, radialized shield. Cells around the entire circumference of the germ ring are stained. (D) Animal pole view of a 6 h embryo, broad shield. Staining is restricted to a  $160^\circ$  arc at the margin. Note that lateral observation of the 6 h embryos shows that staining is restricted to involuted cells. For E-H, the yolks were left intact, and the embryos were photographed in dark field. (E) Oblique animal pole view of 8 h embryos. A ring of hybridization is observed above the germ-ring/yolk margin. (F) Oblique animal pole view of 10 h embryos. Hybridization is just ventral to the animal pole. (G) Lateral view of 14 h embryos. A circular cap of staining occupies the animal pole. (H) Dorsal and anterior views of 10 h late-lithium embryos. While the medial-strip (ms) and medial swelling of the rostral-crescent (rc) patterns are observed, the lateral-wing staining is reduced or absent.

In contrast, at 10 h, while the rostral-crescent swelling and the medial-strip patterns are seen, the lateral-wings are reduced or fully absent (Fig. 8H). Since the cells within these wings occur in the regions that fail to differentiate normally, their absence might be responsible in part for the anterior defects.

Late-lithium exposure could mediate reduced anterolateral *goosecoïd* expression either by inhibiting *goosecoïd* transcription in 'wing' cells, but not in central rostral-crescent or medial-strip cells; or by disrupting cell movements that might direct the anterolateral accumulation of *goosecoïd* cells. To this end, the medial swelling of the crescent projects further anteriorwards and appears to include more cells in 10 h late-lithium versus control embryos (compare Figs 8H and 7F). Furthermore, these embryos are somewhat elongated along their anteroposterior axes as compared to control embryos, suggesting they are undergoing aberrant morphogenetic movements.

## DISCUSSION

### The zebrafish dorsal axis is specified during early development

Our results demonstrate that dorsal cues are present and function in the zebrafish embryo several hours before shield formation, and suggest a rudimentary model of zebrafish axis formation (Fig. 9A). A primary molecular asymmetry in the cleavage-stage embryo, the dorsal determination center or dorsal signal, induces a dorsal fate in overlying blastomeres. These cells express organizer genes at the mid-blastula, and establish a domain within the embryo that organizes the formation and primary patterning of the embryonic axis. During gastrulation, this domain promotes and acts as a focus of mediolateral convergence-extension movements in the epiblast and hypoblast, to build the embryonic shield and axis; it segregates the axial and paraxial mesoderm, which respectively give rise to the prechordal

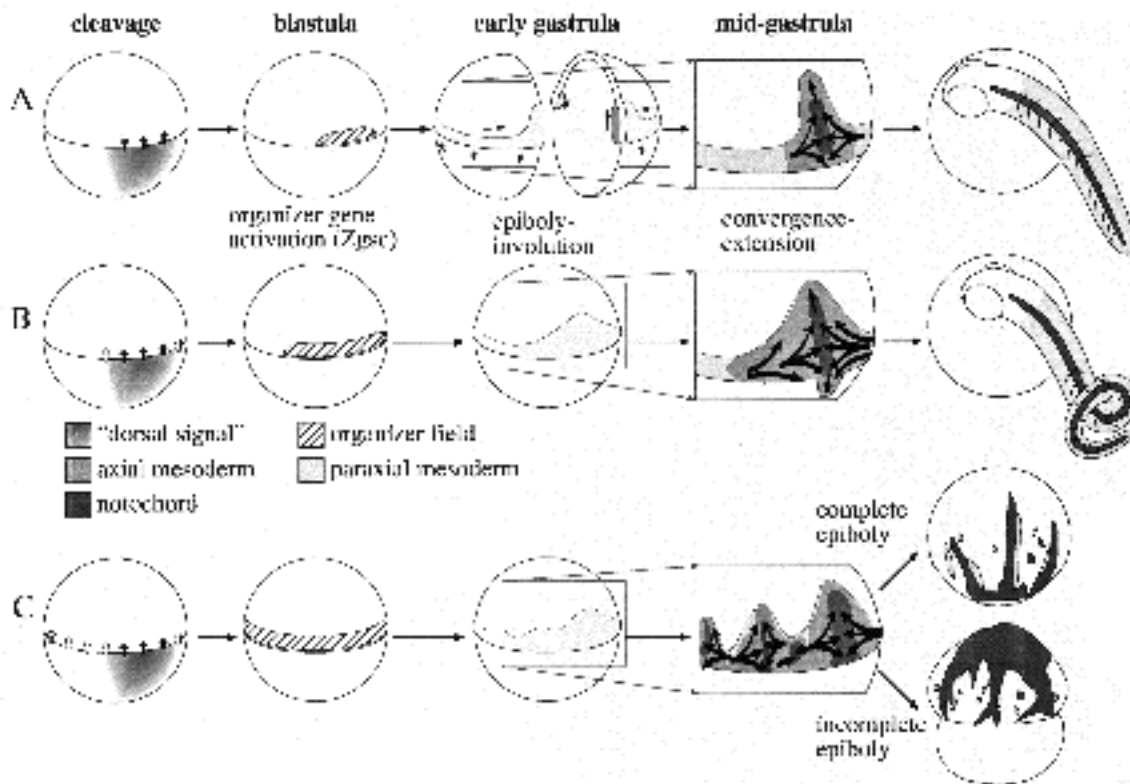


**Fig. 9.** Models of the zebrafish dorsal axis pathway and the lithium-induced generation of the bustled and radialized defects. At cleavage, the closed arrows represent the induction of overlying blastomeres by the dorsal determination center (dorsal signal), and the open arrows represent the dorsalizing effect of lithium on blastomeres outside the normal range of the dorsal signal. At mid-gastrulation, the regions undergoing convergence-extension are shown, which correspond to the boxed areas at early gastrulation. Only the hypoblast is depicted, which has been divided into the axial and paraxial mesoderm; the arrows correspond to convergence-extension movements within the hypoblast. (A) Normal development. The arrows at 6 h represent epiboly, involution and convergence cell movements. (B) Bustled development. (C) Radialized development.

plate and head mesoderm anteriorly, and to the notochord and somites posteriorly. That this model resembles the *Xenopus* dorsal pathway suggests that analogous mechanisms mediate teleost and amphibian axis specification.

Our working hypothesis is that the fish dorsal signal is equivalent to the amphibian Nieuwkoop center, which is generated via the cortical rotation (Vincent and Gerhart, 1987; Houliston and Elinson, 1991) and localized to dorsal vegetal blastomeres (Nieuwkoop, 1973; Gimlich and Gerhart, 1984; Smith and Harland, 1991). Preliminary clues suggest that the fish dorsal signal might also be established and localized in the early embryo. For example, UV irradiation of fertilized one-cell zebrafish, while not disruptive to epiboly or involution, produces embryos that are deficient in or lack dorsal axial structures (D. Kane, personal communication; Stachel, unpublished results). Thus, as in the frog embryo, a microtubule-mediated event during the first cleavage might promote the generation of an asymmetry essential for zebrafish axis determination.

The fish embryo has no obvious cellular equivalent of vegetal blastomeres and, indeed, blastomere extirpation experiments have shown that there is no dorsal determination center in the early blastoderm (Morgan, 1895; Hoadley, 1928). This center might instead be localized to the yolk cell. For example, while a late cleavage-stage blastoderm separated from its yolk develops axial structures, a simi-

larly isolated early cleavage-stage blastoderm, while continuing to divide, fails to differentiate further (Oppenheimer, 1936a; Kostamarova, 1968). Also, the early blastoderm can be rescued by transplanting it onto a cleavage-stage yolk; in contrast, an early blastoderm transplanted onto a gastrula yolk fails to differentiate, even though it undergoes epiboly and involution (Devillers, 1952). These results suggest that the early yolk contains an essential morphogenetic factor, which could correspond to the dorsal determination center of Fig. 9.

#### Action of lithium teratogenesis

Lithium is thought to dorsalize *Xenopus* development by increasing the effective range of the Nieuwkoop center signal. This effect, which appears to be mediated via the inhibitory action of lithium on the PI cycle (Busa and Gimlich, 1989), can result in the induction of dorsal mesoderm throughout the entire marginal zone (Kao and Elinson, 1989). Lithium could similarly dorsalize zebrafish development, and we propose in Fig. 9B and C that lithium causes blastomeres beyond the normal range of the dorsal signal to take on a dorsal fate. If this effect is limited to cells adjoining the normal range of the signal, a broadened organizer field is produced, while a radialized field is generated if cells throughout the blastoderm are dorsalized. The increased organizer tissue leads to excess convergence-

extension, and an excess of axial and a deficit of paraxial mesoderm. Gastrulae with a single broadened organizer develop an expanded and twisted notochord, and gastrulae with a radialized organizer form several foci of convergence-extension, and thus, multiple dorsal axes. If these latter embryos complete epiboly, the supernumerary notochords fuse caudally into a mass of tissue at the blastopore and project upwards; if epiboly is incomplete, the notochords fuse rostrally at the animal pole and project downwards.

Lithium could promote blastomeres to a dorsal fate by mimicking the action of the dorsal signal in them, or by sensitizing them to respond to normally subthreshold levels of signal. We favor this second alternative since *goosecoid* expression in lithiumized embryos often first appears as a gradient across the blastoderm; and shorter and longer times of lithium exposure respectively yield broadened and radialized shields, as if the range of the dorsal signal increases with increased perturbation.

The defective forms produced by lithium also provide new insights into zebrafish morphogenesis. For example, the constriction of the blastopore onto the yolk cell observed in epiboly-deficient embryos suggests that epiboly and blastopore closure might be driven by constriction hoops located at the blastopore, as occurs in *Xenopus* (Keller et al., 1992). Also, the massive posterior extensions that form in lithiumized embryos suggest that convergence-extension movements can occur independently of normal underlying substratum, and thus might be driven by autonomous forces, as found in *Xenopus* and other anuran, but not in urodele, gastrulae (Keller et al., 1985; Shi et al., 1987).

### **goosecoid expression**

The pattern of *goosecoid* expression in normal and perturbed embryos is characteristic of a gene that might function in the establishment and maintenance of the organizer. *goosecoid* expression is locally activated at or just after the midblastula, marks the cells that first involute and converge to build the nascent shield, is restricted to the anterior axial hypoblast throughout gastrulation, is globally activated and radialized in embryos that develop radialized shields, and is reduced by perturbations that limit shield formation and yield ventralized embryos. Transplantation experiments have led to the proposal that the anterior and posterior regions of the shield express distinct 'head' and 'trunk' organizer functions (Eakin, 1939; Oppenheimer, 1955). The anterior localization of *goosecoid* transcripts suggests that zebrafish *goosecoid* might be specifically associated with the head organizer, as has been proposed for *Xenopus goosecoid* (Cho et al., 1991).

While zygotic *goosecoid* transcripts are first localized to a patch that extends from the margin towards the animal pole, by the late-blastula *goosecoid* expression is restricted to the margin. This phenomenon, which is particularly apparent in lithiumized embryos, could be produced by a downward migration and aggregation of *goosecoid* cells. Alternatively, this secondary localization could be due to *goosecoid* being regulated by two signals - the dorsal signal, which first activates expression, and a second signal localized around the margin, which is essential for the mainte-



**Fig. 10.** Model of hypoblast cell movements that generate the rostral crescent. An animal pole view of the hypoblast is diagrammed. The black arrows represent the anterior axial cells, which express *goosecoid*; the anterior and posterior regions of this pattern respectively correspond to the rostral crescent and medial strip, and the arrowheads represent the

medial swelling and lateral wings of the crescent. The gray arrows correspond to migrating lateral and ventral cells. The caudal deflection of axial cells at the animal pole (+) has been exaggerated.

nance of expression. Our results would suggest that lithium perturbs the dorsal but not the marginal signal. To distinguish between these models, we are pursuing methods to label and follow *goosecoid* cells in living embryos.

*goosecoid* expression in the late gastrula describes a complex pattern of the rostral crescent and medial strip (Fig. 10). The crescent is dorsal to the strip, which is completely anterior to and in the plane of the notochord. That *goosecoid* expression is continuous between the crescent and strip suggests that they belong to a single cell population and our working hypothesis is that the crescent is produced by the directed rearrangement of cells within the anterior portion of the medial strip (Fig. 10). In fish gastrulation, cells involute from around the entire blastoderm and migrate toward the animal pole. As dorsal, lateral and ventral cells give rise to distinct tissues, they should not intermix. To achieve this, cells of each population could have a higher affinity for each other than for other cells. To this end, Trinkaus et al. (1992) have shown that dorsal hypoblast cells in the *Fundulus* gastrula migrate in monolayer clusters maintained by adhesive contacts and movement of these clusters is contact inhibited. Thus, instead of intercalating with lateral and ventral hypoblast at the animal pole, anterior dorsal axial cells could actively be deflected caudally and laterally to generate the rostral crescent. That this pattern is uniform from embryo to embryo suggests that such cellular interactions might play a significant role in anterior morphogenesis.

S. E. S. thanks Richard Harland for essential advice and protocols on immunohistochemistry and in situ hybridization, for suggesting the *goosecoid* experiments, for facilities, and for continued enthusiasm; Ali Hemmati-Brivanlou for a *Xenopus goosecoid* cDNA plasmid and oligonucleotides; Fiona Watt, Frank Stockdale, Nipam Patel and Ruth BreMiller for antibodies; Kathryn Helde for the zebrafish cDNA library; Robert Weiss for his mini-transposon system and Kerry Dew-Jager for assistance with thermocycle DNA sequencing; Shige Sakonju, Carl Thummel and Ray Gesteland for generous sharing of reagents and facilities; Tabitha Doniach, Richard Elinson, Richard Harland, Ray Keller and Chuck Kimmel for discussions; and Ernest T. Wombatt III for comments. P. Z. M. thanks Michael Bastiani for support. This work was supported by ACS, NSF and University of Utah grants to D. J. G. and S. E. S. was supported by a Cancer Training Grant. D.J.G. is a recipient of a Basil O'Connor Starter Scholarship Award and a Sloan fellowship.

## REFERENCES

- Bäckström, S. (1954). Morphogenetic effects of lithium on the embryonic development of *Xenopus*. *Arkiv. Zool.* **6**, 527-526.
- Berridge, M. J., Downes, C. P. and Hanley, M. R. (1989). Neural and developmental actions of lithium: a unifying hypothesis. *Cell* **59**, 411-419.
- Blum, M., Gaunt, S. J., Cho, K. W. Y., Steinbeisser, H., Blumberg, B., Bittner, D. and De Robertis, E. M. (1992). Gastrulation in the mouse: the role of the homeobox gene *gooseoid*. *Cell* **69**, 1097-1106.
- Blumberg, B., Wright, C. V. E., De Robertis, E. M. and Cho, K. W. Y. (1991). Organizer-specific homeobox genes in *Xenopus laevis* embryos. *Science* **253**, 195-196.
- Busa, W. B. and Gimlich, R. L. (1989). Lithium-induced teratogenesis in frog embryos prevented by a polyphosphinositide cycle intermediate or a diacylglycerol analog. *Dev. Biol.* **132**, 315-324.
- Carroll, R. L. (1988). *Vertebrate Paleontology and Evolution*. New York: W. H. Freeman and Company.
- Cho, K. W. Y., Blumberg, B., Steinbeisser, H. and De Robertis, E. M. (1991). Molecular nature of Spemann's organizer: the role of the *Xenopus* homeobox gene *gooseoid*. *Cell* **67**, 1111-1120.
- Cooke, J. and Smith, E. J. (1988). The restrictive effect of early exposure to lithium upon body pattern in *Xenopus* development studied by quantitative anatomy and immunofluorescence. *Development* **102**, 85-99.
- Davidson, E. H. (1990). How embryos work: a comparative view of diverse modes of cell fate specification. *Development* **108**, 365-389.
- Devillers, C. (1952). Coordination des forces épiboliques dans la gastrulation de *Salmo*. *Bull. Soc. Zool. Fr.* **77**, 304-309.
- Dirksen, M. L. and Jamrich, M. (1992). A novel, activin inducible, blastopore lip-specific gene of *Xenopus laevis* contains a fork head DNA-binding domain. *Genes Dev.* **6**, 599-608.
- Eakin, R. M. (1939). Regional determination in the trout. *Wilhelm Roux's Arch. EntMech. Org.* **139**, 274-281.
- Elinson, R. P. and Rowning, B. (1988). A transient array of parallel microtubules in frog embryos: potential tracks for cytoplasmic rotation that specifies the dorso-ventral axis. *Dev. Biol.* **126**, 185-197.
- Gerhart, J., Danilchik, M., Doniach, T., Roberts, S., Rowning, B. and Stewart, R. (1989). Cortical rotation of the *Xenopus* egg: consequences for the anteroposterior pattern of embryonic dorsal development. *Development* **107** Supplement, 37-51.
- Gimlich, R. L. and Gerhart, J. C. (1984). Early cellular interactions promote embryonic axis formation in *Xenopus laevis*. *Dev. Biol.* **104**, 117-130.
- Harland, R. M. (1991). *In situ* hybridization: an improved whole mount method for *Xenopus* embryos. *Methods in Cell Biology* **36**, 675-685.
- Hart, D. and Donavon, M. (1983). The structure of the chorion and site of sperm entry in the egg of *Brachydanio*. *J. Exp. Zool.* **227**, 277-296.
- Hatta, K., BreMiller, R., Westerfield, M. and Kimmel, C. B. (1991). Diversity of expression of engrailed-like antigens in zebrafish. *Development* **112**, 821-832.
- Hemmati-Brivanlou, A. and Harland, R. M. (1989). Expression of an engrailed-related protein is induced in the anterior neural ectoderm of early *Xenopus* embryos. *Development* **106**, 611-617.
- Hoadley, L. (1928). On the localization of developmental potencies in the embryo of *Fundulus heteroclitus*. *J. Exp. Zool.* **52**, 7-44.
- Houliston, E. and Elinson, R. P. (1991). Patterns of microtubule polymerization relating to cortical rotation in *Xenopus laevis* eggs. *Development* **112**, 107-117.
- Kao, K. R. and Elinson, R. P. (1986). Lithium-induced respecification of pattern in *Xenopus laevis* embryos. *Nature* **322**, 371-373.
- Kao, K. R. and Elinson, R. P. (1988). The entire mesodermal mantle behaves as Spemann's organizer in dorsoanterior enhanced *Xenopus laevis* embryos. *Dev. Biol.* **127**, 64-77.
- Kao, K. R. and Elinson, R. P. (1989). Dorsalization of mesoderm induction by lithium. *Dev. Biol.* **132**, 81-90.
- Keller, R., Shih, J. and Domingo, C. (1992). The patterning and functioning of protusive activity during convergence and extension of the *Xenopus* organizer. *Development* **1992** Supplement, in press.
- Keller, R. E., Danilchik, M., Gimlich, R. and Shih, J. (1985). The function and mechanism of convergent extension during gastrulation of *Xenopus laevis*. *J. Embryol. Exp. Morph.* **89** Supplement, 185-209.
- Kimmel, C. B., Warga, R. M. and Schilling, T. F. (1990). Origin and organization of the zebrafish fate map. *Development* **108**, 581-594.
- Kostomarov, A. A. (1969). The differentiation capacity of isolated loach (*Misgurnis fossilis* L.) blastoderm. *J. Embryol. Exp. Morphol.* **22**, 407-430.
- Luther, W. (1935). Potenzprüfungen an isolierten teilstücken der forellenkeimscheibe. *Wilhelm Roux's Arch. EntwMech. Org.* **135**, 359-383.
- Maslanski, J. A., Leshko, L. and Busa, W. B. (1992). Lithium-sensitive production of inositol phosphates during amphibian embryonic mesoderm induction. *Science* **256**, 243-245.
- Miller, J. B., Crow, M. T. and Stockdale, F. E. (1985). Slow and fast myosin heavy chain content defines three types of myotubes in early muscle cell cultures. *J. Cell Biol.* **101**, 1643-1650.
- Morgan, T. H. (1895). The formation of the fish embryo. *J. Morph.* **10**, 419-472.
- Nieuwkoop, P. D. (1973). The 'organizer center' of the amphibian embryo: its origin, spatial organization, and morphogenetic action. *Adv. Morphogenet.* **10**, 1-39.
- Oppenheimer, J. M. (1936a). The development of isolated blastoderms of *Fundulus heteroclitus*. *J. Exp. Zool.* **72**, 247-269.
- Oppenheimer, J. M. (1936b). Transplantation experiments on developing teleosts (*Fundulus* and *Perca*). *J. Exp. Zool.* **72**, 409-436.
- Oppenheimer, J. M. (1936c). Structures developed in amphibians by implantation of living fish organizer. *Proc. Soc. Exp. Biol. N. Y.* **34**, 461-463.
- Oppenheimer, J. M. (1955). The differentiation of derivatives of the lower germ layers in *Fundulus* following the implantation of shield grafts. *J. Exp. Zool.* **129**, 525-559.
- Patel, N. H., Martin-Blanco, E., Coleman, K. G., Poole, S. J., Ellis, M. C., Kornberg, T. B. and Goodman, C. S. (1989). Expression of engrailed proteins in arthropods, annelids and chordates. *Cell* **58**, 955-968.
- Regen, C. M. and Steinhardt, R. A. (1988). Lithium dorsalizes but also mechanically disrupts gastrulation of *Xenopus laevis*. *Development* **102**, 677-686.
- Scharf, S. R. and Gerhart, J. C. (1983). Axis determination in eggs of *Xenopus laevis*: a critical period before first cleavage, identified by the common effects of cold, pressure, and ultraviolet irradiation. *Dev. Biol.* **99**, 75-87.
- Shi, D.-L., Delarue, M., Darribere, T., Riou, J.-F. and Boucaut, J.-C. (1987). Experimental analysis of the extension of the dorsal marginal zone in *Pleurodeles waltl* gastrulae. *Development* **100**, 147-161.
- Smith, J. C. and Watt, F. M. (1985). Biochemical specificity of *Xenopus* notochord. *Differentiation* **29**, 109-115.
- Smith, W. C. and Harland, R. M. (1991). Injected Xwnt-8 RNA acts early in *Xenopus* embryos to promote formation of a vegetal dorsalizing center. *Cell* **67**, 753-765.
- Smith, W. C. and Harland, R. M. (1992). Expression cloning of *noggin*, a new dorsalizing factor localized to the Spemann organizer in *Xenopus* embryos. *Cell* **829**-840.
- St. Johnston, D. and Nüsslein-Volhard, C. (1992). The origin of pattern and polarity in the *Drosophila* embryo. *Cell* **68**, 201-219.
- Stewart, R. M. and Gerhart, J. C. (1990). The anterior extent of dorsal development of the *Xenopus* embryonic axis depends on the quantity of organizer in the late blastula. *Development* **109**, 363-372.
- Taira, M., Jamrich, M., Good, P. J. and Dawid, I. B. (1992). The LIM domain-containing homeo box gene *Xlim-1* is expressed specifically in the organizer region of *Xenopus* gastrula embryos. *Genes Dev.* **6**, 356-366.
- Trearrow, B., Marks, D. L. and Kimmel, C. B. (1990). Organization of hindbrain segments in the zebrafish embryo. *Neuron* **4**, 669-679.
- Trinkaus, J. P., Trinkaus, M. and Fink, R. D. (1992). On the convergent cell movements of gastrulation in *Fundulus*. *J. Exp. Zool.* **261**, 40-61.
- Vincent, J.-P. and Gerhart, J. C. (1987). Subcortical rotation in *Xenopus* eggs: an early step in embryonic axis specification. *Dev. Biol.* **123**, 526-539.
- Warga, R. M. and Kimmel, C. B. (1990). Cell movements during epiboly and gastrulation in zebrafish. *Development* **108**, 569-580.
- Westerfield, M. (1989). *The Zebrafish Book*. Eugene, OR: Univ. Oregon Press.
- Yamaguchi, Y. and Shinagawa, A. (1989). Marked alteration at midblastula transition in the effect of lithium on formation of the larval body plan of *Xenopus laevis*. *Dev. Growth and Differ.* **31**, 531-541.